

Evaluation of the Mechanical and Tribological Properties of A6061 Reinforced Hybrid Metal Matrix Composites with B₄C and Gr

Mr. Pavan Chaudhary
Assistant Professor, Mechanical
Engineering Department,
Maharishi University of Information Technology Maharishi University of Information Technology

Mr. Sanjaya Kumar
Research Scholar,
M.Tech.Production Engineering
Maharishi University of Information Technology

Abstract: Aluminum alloy (A6061)-based hybrid metal matrix composites (HMMCs) are produced through a dual stir casting technique, incorporating varying volume percentages of B₄C (5%, 10%, and 15%) and Gr (10%, 15%, and 20%). These HMMCs and reinforcement components are evenly distributed within the primary matrix, forming a mechanically mixed layer with interfacial reactions. This layer reduces wear loss and friction coefficient compared to A6061, particularly with higher levels of B₄C and Gr, which exhibit minimal aggregation of reinforced material. The presence of Gr particles allows for the integration of different wear parameters (applied load, sliding speed, and distance). Micro-hardness investigations reveal an increase in HMMC hardness with rising volume fractions of reinforced particles and sliding distance. Compression testing demonstrates a 22% enhancement over Al6061, indicating that incorporating reinforcing materials into the matrix enhances strength by boosting wear resistance, aided by Gr's lubricating effect

Keywords: hybrid metal matrix composites; stir casting method; wear behavior; microstructural characteristic; aluminum alloys

1. Introduction

Aluminum alloy (A6061) metal matrix composites (MMC) offer numerous advantages over heavy ferrous metals, including lightweight construction, high specific strength, elastic modulus, improved high-temperature performance, and enhanced antifriction behavior [1]. In recent years, hybrid composites like Al6061 matrix reinforced with B₄C have gained prominence due to their superior mechanical and tribological properties, resulting from the synergistic effects of their constituent materials [2]. B₄C,

renowned for its high hardness, stiffness and low density, proves to be an effective reinforcing material when combined with AA, resulting in a high-specific-strength product with superior wear resistance and thermal stability. However, achieving proper wetting between B₄C particulates and molten AA at low temperatures poses a challenge, yet is essential for enhancing mechanical and physical properties such as stiffness, density, wear resistance, and hardness [3]. Studies have shown that using larger particle sizes of B₄C leads to improved microstructures without particle agglomeration [4]. Moreover, investigations into the interface of B₄C particle-reinforced A2024 MMCs have revealed a refined microstructure with sub-grains as small as 400 nm [5]. Additionally, AA-B₄C composites produced through accumulative roll bonding exhibit a uniform dispersion of B₄C particles in the aluminum matrix [6]. These advancements underscore the significant potential of incorporating reinforcing materials into AA matrices to enhance strength and wear resistance. The study on the sliding wear behavior of cast A6061 composites reveals that as the volume percentage of Al₂O₃ particles increases, both heat conductivity and friction coefficient decrease [8]. Furthermore, it was observed that the level of porosity does not influence the wear rate (WR) of the composites. However, in AA composites reinforced with B₄C, titanium boride, and silicon nitride ceramics, an increase in porosity leads to a decrease in hardness [9].

The introduction of graphite (Gr) into A6061 enhances wear resistance but compromises the mechanical strength of AA, despite Gr's inherent low strength [10]. On the other hand, the incorporation of B₄C into A6061 enhances corrosion resistance [11]. In the examination of A7075-SiC with neem leaf ashes, it was found that wear resistance decreases while material strength increases due to the presence of silicon carbide [12]. The addition of carbon nanoparticles to AA 7075 induces significant changes in microstructure, resulting in notable improvements in mechanical properties such as tensile and compression strength [13].

Hybrid AA matrix composites reinforced with Gr and SiC particulates exhibit superior wear characteristics along with enhanced mechanical properties [14]. Furthermore, the addition of 10% B₄C in AA MMC enhances mechanical strength while reducing the wear rate [15]. The tribological behavior of A6061 was investigated by adjusting the weight percentages of carbon nanotube (CNT) and SiC using the stir casting process (SCP) [16]. Additionally, the friction behavior of Al 6061-SiC-MWCNT was found to be significantly influenced by variations in load [17]. An analysis conducted using a scanning electron microscope (SEM) on wear track microstructures of A5052 reinforced with 5% tungsten carbide demonstrated that the addition of tungsten carbide reduced wear while maintaining constant input parameters [18]. Another study examined A6061- B₄C powders with varying concentrations of B₄C (5, 10, and 15 wt.%) at 5% Gr, highlighting that the sample containing 15 wt.% B₄C exhibited superior wear

characteristics, displaying a hardness value of 164 HV, notably higher than the 33 HV observed for pure AA. It was noted that the coefficient of friction was affected by load and sliding speed, with higher loads and sliding speeds correlating with increased friction. Additionally, the stir casting process (SCP) was identified as more cost-effective compared to alternative treatments, costing thirty times less [19].

Investigations into the wear characteristics of hyper eutectic Al-silicon alloys produced through partial solid metal processing were conducted under specific conditions of 0.2 m/s sliding rate and 10–40 N load, with prolonged cooling on steel and cast iron wheels. Using borax as a wet medium mixed with 50% SiC after heating at 250°C for 20 minutes resulted in a smooth dispersion of SiC [20].

Furthermore, a dual-phase MEA, consisting of (CoCrNi)₈₈Mo₁₂, was developed with the intention of enhancing cryogenic wear performance. This material exhibited a friction-induced amorphous layer that reduced wear by 73% at 113 K [21].

The tribological behavior of a hydrocarbon compound produced with 2.5% to 10% equivalent weight of SiC and graphite (Gr) particles was analyzed using design of experiments approaches, demonstrating that wear was influenced by favorable parameters such as force and sliding distance [22].

Lastly, the dry-sliding wear behavior of AA reinforced with 5% SiC and B₄C hybrid was explored using a pin-on-disk tribometer (PODT). These hybrid composites maintained their resistance qualities under 60 N loads and falling rate ranges of 1–4 m/s. The collaborative effect of reinforcement particles contributed to enhanced wear resistance with a small amount of SiC and B₄C [23]. Additionally, SCP was employed to synthesize various weight percentages of B₄C and a constant 3% of BN reinforcements in A-7075 HC, leading to increased micro-hardness, tensile strength, compression, and reduced corrosion rates by 18.5% to 22.4% [24].

Incorporating B₄C ceramic along with graphite (Gr) into aluminum-based metal matrix composites (MMCs) via stir casting process (SCP) has been shown to elevate micro-hardness while reducing weight loss (WL) with increasing concentrations of B₄C and graphite. Optimal wear resistance was observed at 15 wt.% B₄C and 10 wt.% Gr [25].

Response surface analysis (RSM) and artificial neural network (ANN) techniques were employed to evaluate the impact of tests and determine their significance levels. The Taguchi model, coupled with

ANN, was utilized to understand the wear behavior of the hybrid mixture and estimate the influential factors affecting the degradation rate of composites [26].

Although limited data exists on the effects of dry sliding wear on multi-ceramic reinforced composites, insights from this research will contribute to defining the role of hybridized composites (Al6061 + B₄C + Gr) in practical applications [27,28].

The incorporation of Gr particles into aluminum alloys has been found to notably enhance wear resistance and decrease the coefficient of friction. Additionally, the formation of a tribo-layer on the composite surface enhances material integrity by providing lubrication [29].

In composites comprising 40% SiC/5% Gr/AA with varied sizes of graphite particles using the squeeze casting method, the inclusion of Gr particles led to a decrease in the friction coefficient and a significant increase in wear resistance by a substantial margin of 170 to 340 times. Moreover, wear resistance showed an upward trajectory with increasing graphite particle size, indicating improved lubricating properties [30].

Aluminum-based hybrid metal matrix composites (HMMCs) have garnered significant attention in industries such as automotive and aerospace due to their enhanced mechanical properties, including increased strength, hardness, stiffness, wear and corrosion resistance, and favorable thermal characteristics. To further improve these properties and mitigate certain challenges, such as brittleness and machinability issues, boron carbide (B₄C) and graphite (Gr) are commonly added to aluminum HMMCs. B₄C helps enhance wear resistance, while Gr aids in addressing the strength reduction typically associated with Gr-reinforced composites.

Despite existing research in the field, there is a lack of comprehensive guidance on utilizing the dual-stage stir casting process (SCP) for effectively incorporating variable volume percentages of B₄C and Gr into an Al-6061 alloy matrix, especially when previous attempts involved insufficient volume percentages. This knowledge gap hampers our ability to fully understand the morphological, hardness, and tribological characteristics of these composites.

By adjusting the volume percentages of Gr, which possesses moderately lubricating properties but is brittle in nature, it is possible to further enhance the mechanical and tribological behavior of AA-MMCs. In this study, our objective was to manufacture B₄C- and Gr-reinforced Al6061 hybrid composites by varying their volume percentages (5%, 10%, and 15% for B₄C, and relatively higher amounts of 10%, 15%, and 20% for Gr) using the dual-stage SCP method. Additionally, we aimed to analyze the

morphological, mechanical, and tribological behavior of these composites under various parameter conditions.

2. Materials and Methodology

In this study, A6061 alloy was selected as the matrix for producing aluminum-based hybrid composites (HCs) using the stir casting process (SCP). A6061 alloy possesses several desirable properties, including a high strength-to-weight ratio, adequate strength, low density, cost-effectiveness, and exceptional quality, making it widely utilized in automotive and marine applications (see composition Table 1). By incorporating low-density reinforcements such as B₄C (with a density of 2500 kg/m³ and particle size of 1 μm) and Gr (with a density of 2100 kg/m³ and particle size of 10 μm), the density of the resulting HC can be reduced compared to A6061 (with a density of 2700 kg/m³) and other ceramic-reinforced materials. Furthermore, combining B₄C and Gr with aluminum can enhance properties such as high thermal conductivity, excellent workability, and machinability.

The addition of these reinforcing components in varying volume percentages improves specific physical characteristics of the aluminum-based HCs, such as a high strength-to-weight ratio, reduced density, increased stiffness, and enhanced lubrication. Gr enhances the wear resistance of the HC, particularly at elevated temperatures, while B₄C exhibits wettable, thermally stable, and chemically inert properties. In this study, aluminum-based HCs were fabricated with different percentages of B₄C (5%, 10%, and 15%) and Gr (10%, 15%, and 20%) in higher content. Notably B₄C is a stiffer material compared to Gr, and the presence of Gr facilitates good bonding to aluminum, promoting microstructural uniformity and stability.

The scanning electron microscope (SEM) microstructure images of the raw B₄C and Gr materials are depicted in Figure 1a and 1b, respectively. Figure 1a illustrates the topographic SEM image of B₄C particles, exhibiting flat, hexagonal platelet shapes with sizes ranging from 1 to 2 μm, and devoid of other detectable elements. Conversely, Figure 1b displays Gr powder particles with sizes ranging from 9 to 10 μm, appearing agglomerated and presenting irregular shapes resembling flakes of varying sizes.

At both high and extremely low temperatures, A6061 alloy demonstrates strength and resistance to damage. In this study, pure A6061 and three types of composites (A6061/ B₄C /Gr) were developed. A6061 alloy exhibits tensile and yield strengths of 290 MPa and 248 MPa, respectively [34].

Table 1. Composition of Al6061 HC in wt.%.

Mg	Cu	Si	Ti	Fe	Mn	Al
----	----	----	----	----	----	----

0.84	0.33	0.76	0.02	0.14	0.29	97.61
------	------	------	------	------	------	-------

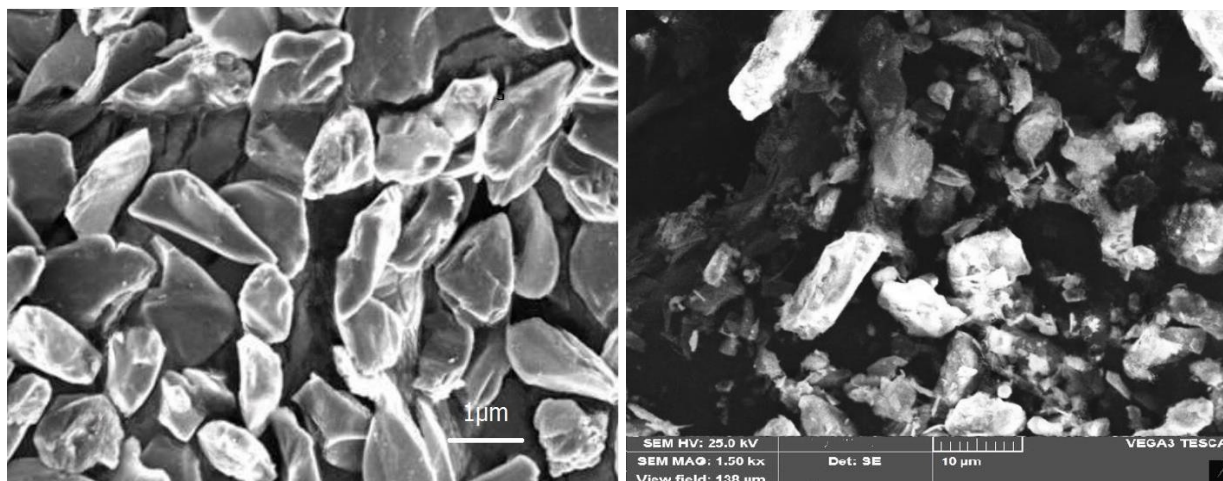


Figure 1. Morphological view of (a) B₄C (b) Gr.

The stir casting process (SCP) has emerged as one of the most cost-effective methods for manufacturing Metal Matrix Composites (MMCs), particularly aluminum-based hybrid composites (Al-HCs). In this study, Gr and B₄C materials underwent a thorough cleaning process using water and were subsequently heated to 200°C and 600°C, respectively. This heating step served to eliminate any dust, moisture, or carbonaceous residues, ensuring the purity of the materials. Once the materials changed color from black to grey, indicating readiness, they were considered prepared for use in the main manufacturing procedure.

The manufacturing process involved a dual stirring casting method, where specimens containing 85%, 75%, and 65% A6061 were produced at a molten temperature of 750°C. Preheated Gr (at concentrations of 10%, 15%, and 20%) and B₄C (at concentrations of 5%, 10%, and 15%) were then added to the slurry at a consistent pace, ensuring uniform distribution of reinforcing particles. This step was crucial for achieving critical features in both elements, including volume, shape, and location within the composite structure.

The mixture underwent agitation for approximately 5–10 minutes to ensure thorough mixing of all ingredients. Subsequently, the slurry was poured into molds and stored at 450°C for 45 minutes to facilitate uniform solidification. Transferring the produced Al-HC slurry into preheated steel dies, maintained at 350°C, and allowing it to cool to ambient temperature helped prevent heterogeneity and facilitated controlled cooling, ensuring the quality and integrity of the final product.

Micro hardness Tests of A6061/ B₄C /Gr:

The Vickers micro-hardness tester, following the guidelines outlined in ASTM E384-10, was employed to evaluate the hardness of the samples. Micro-hardness tests were conducted on both the A6061 alloy and its composites at a speed interval of 2 m/s. Initially, the pin surface was prepared to achieve a surface finish of 0.3 μm using finer diamond abrasives. Subsequently, all samples underwent a 500 g load for 10 seconds. To ensure accuracy and minimize the likelihood of the indenter resting on hard reinforcement particles, the test was performed at five distinct locations [37].

Density Measurement:

The mass density of both the unreinforced AA and Al HCs was determined based on Archimedes' principle. Initially, the specimen was suspended freely in the air and weighed. Then, it was fully immersed in distilled water, and its mass was determined again. Since the mass of the specimen fully immersed in water is less than its mass in air, the mass density (kg/m^3) of the specimen was calculated using the following expression [33]:

$$\rho = \frac{m_1}{m_1 - m_2} \times \rho_w$$

where m_1 and m_2 are the specimen's masses in air and water (kg/m^3), and ρ_w is the mass density of water. Whereas the theoretical density (ρ_{com}) was evaluated by using expression (2) with V as total volume of composite:

$$\rho_{com} = \frac{m_1}{V} + \frac{m_2}{V} + \frac{m_3}{V}$$

The compressive strength of the AA matrix material reinforced with its corresponding reinforcement was determined following ASTM-E9 guidelines [38]. Specimens were prepared with dimensions of 5 x 3 x 3 mm^3 and subjected to compression testing using an INSTRON 5985 model computerized universal testing machine. The test was conducted at room temperature with a crosshead speed of 0.5 mm/min. Each specimen was compressed up to 25% of its initial height, and the applied force corresponding to this deformation was recorded [39]. Five specimens were tested in total.

For the morphological evaluation of the produced Al-MMCs and a deeper understanding of their microstructural properties, samples were prepared for metallography following ASTM standards.

The microstructural pattern of the HC samples was examined using a scanning electron microscope (SEM) (Make: VEGA 3 TESCAN, Brno, Czech Republic). Prior to SEM analysis, the samples were etched using Keller's reagent ($\text{HCl} + \text{HF} + \text{HNO}_3$) to reveal the distribution of particles (B_4C and Gr) in the HCs.

Dry sliding wear tests were conducted using an Al HC pin specimen with a diameter of 12 mm and a length of 30 mm, following the ASTM-G99 standard [40]. The pin was held against a revolving disk face made of EN31 steel with a track diameter of 60 mm. The pin sample surfaces were treated with emery (80 grit size) to ensure cleanliness and horizontal alignment of the contact faces. Before and after each test, both the specimens and the used tracks were cleaned with acetone. The tests were conducted under varying loads (10, 20, and 40 N), speeds (2 and 4 m/s), and sliding distances (2000 m, 4000 m, and 8000 m) [3, 37, 41].

3. Results and Discussion

By adjusting the weight percentages of B_4C and Gr in the stir casting process, B_4C - and Gr-reinforced AA-HCs were successfully manufactured in this study. The present paper aims to examine and investigate the microstructure, hardness, tribological characteristics, worn surface morphology, and compressive strength of the produced HCs.

The morphological characterization of B_4C and Gr reinforced Al-HCs is depicted in Figure 2a–c, which shows SEM images of cast samples after etching, revealing the wear surfaces of A6061/5% B_4C /10% Gr, 10% B_4C /15% Gr, and 15% B_4C /20% Gr HC at specified magnifications using a scanning electron microscope (VEGA 3 TESCAN, Czech Republic). Microstructural analysis of these specimens indicates that B_4C and Gr reinforcements are uniformly distributed across the cross-section of the AA-MMC.

The reinforced particles were observed to cluster in specific areas and along the grain boundaries of the main A6061 matrix, displaying a smooth interdendritic arrangement with precipitated reinforcing particles at the grain boundary junctions. The distribution of the black-colored reinforcing particles, which are opaque and do not reflect light, within the reflective A6061 matrix, was evident in the HC specimens. Additionally, the Gr particles appeared to have a regular granular form [13].

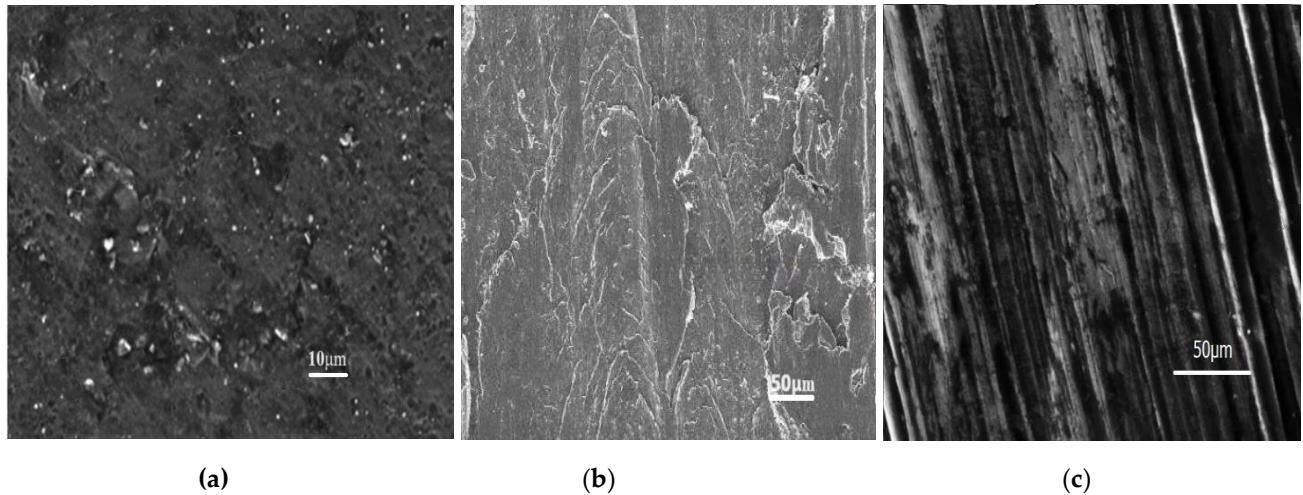


Figure 2 illustrates the microstructural view of A6061+ with varying percentages of B₄C and Gr: (a) 5% B₄C /10% Gr, (b) 10% B₄C /15% Gr, and (c) 15% B₄C /20% Gr HCs.

Upon examination, it was observed that numerous reinforcing particles formed around the peripheries of the main aluminum matrix granules. In contrast, only a few small spotted particles initiated the granule peripheries in the AA matrix [33, 37]. Despite the increasing melt temperature, the reinforcing particles did not fully dissolve; instead, they appeared as small, round-type reinforcing particles in specific regions, with a regular distribution in the AA matrix alloy, as depicted in Figure 2a–c. These reinforcing particles exhibit higher hardness and melting points compared to the AA matrix. However, unmelted reinforcing particles play a significant role in determining the compression intensity of HCs by acting as a damping mechanism.

The HC's dendritic aluminum matrix contains spherical B₄C particles and slightly skewed Gr particles. The distribution patterns of the reinforced particles were found to be randomly oriented [42, 43]. Additionally, Figure 3 illustrates the Energy Dispersive X-ray Spectroscopy (EDS) results of the HMMC composite, confirming the presence of Mg and Si grains in A6061, while other elements such as Gr and B₄C are not visible, indicating a phase change.

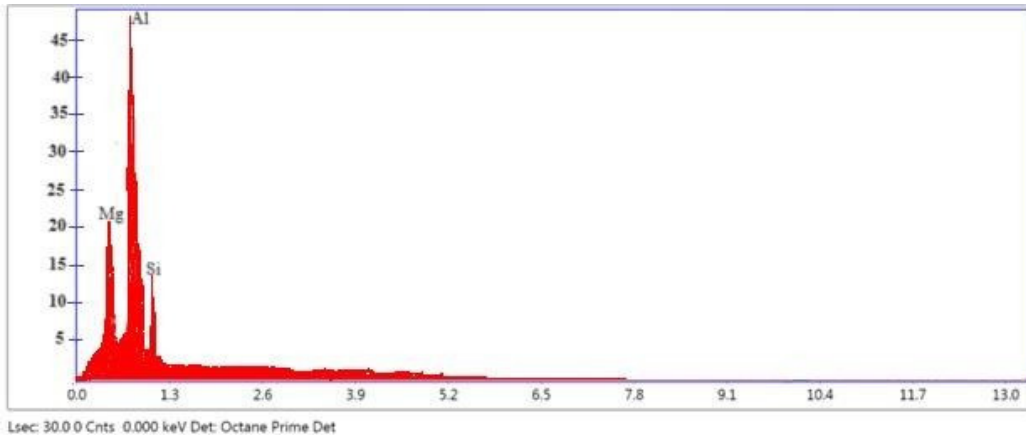


Figure 3. EDS results of A6061 + 15% B₄C /20% Gr HCs after stir casting.

Figure 4 presents the average values obtained from Vickers micro hardness tests conducted on both cast and HC samples. The uniform dispersion of B₄C and Gr in the AA matrix alloy, along with the alteration in granules observed in the micro structural view, indicates the increased hardness of the produced HCs. It was found that a higher weight percentage of B₄C acts as a barrier to disarticulation, resulting in greater hardness compared to AA [25].

The hardness achieved by varying the sliding distance was analyzed at each of these distances to determine which HC exhibits superior wear properties with different weight percentages of Gr and B₄C particles.

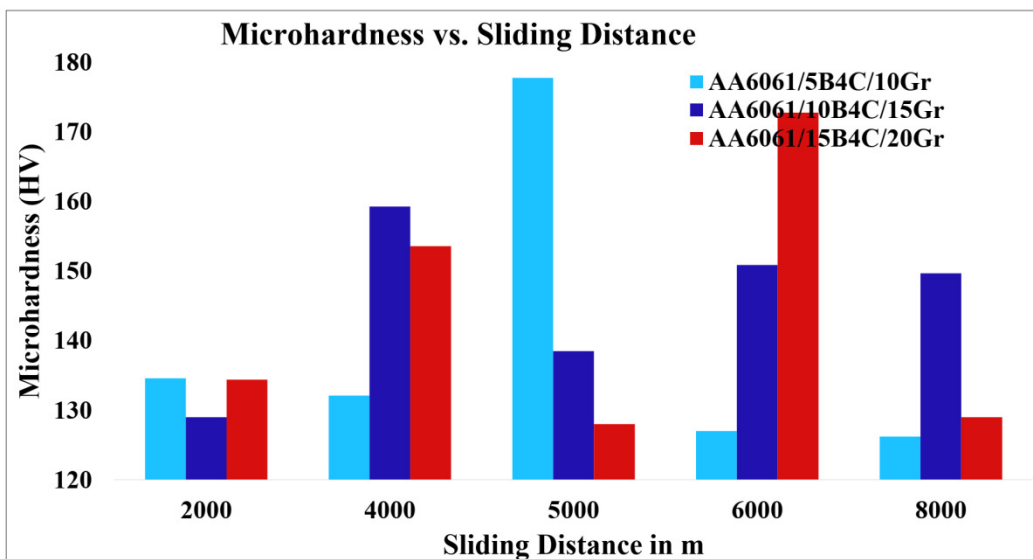


Figure 4. Micro hardness of A6061/ B₄C /Gr with varying combinations of B₄C (5, 10, and 15%) and Gr (10, 15, and 20%) HCs vs. sliding distance.

The micro hardness of A6061/ B₄C /Gr composites exhibited an upward trend with increasing sliding distance up to 5000 m, followed by a subsequent decline and eventual stabilization after reaching 6000 m [27]. This shift in behavior was attributed to initial strain hardening, succeeded by softening due to wear and the accumulation of debris from the reinforcements. The formation of a transfer layer on the worn surface, known as the mechanically mixed layer (MML), contributed to this effect by enhancing micro hardness values. However, as the sliding distance increased, the saturation of the MML led to the stabilization of micro hardness levels.

Additionally, micro hardness decreased due to matrix deformation, fracture of B₄C and Gr particles, and wear-induced damage [34]. The proportion of reinforcements also played a role in influencing micro hardness values, with B₄C content ranging from 5% to 15% and Gr content ranging from 10% to 20%. Smaller particle sizes of B₄C and finer particle sizes of Gr significantly improved hardness. The observed increase in hardness of the composite was primarily attributed to the high hardness of B₄C reinforcing particles, their uniform distribution within the composites, and increased density [42].

The higher observed hardness value can be attributed to the dispersion of Gr and B₄C particulate matter, as evidenced by the uniform dispersion of B₄C particulate matter in the AA matrix and the reinforcing effect of the MMC. The presence of rigid reinforcement particulate matter helps prevent plastic deformation, thereby enhancing the hardness of the metal matrix when combined with the optional inclusion of particulate matter in the composites. Among the compositions investigated, the A6061 + 10% B₄C + 15% Gr composite exhibited the highest hardness value.

The sliding distance (SD) impacts the distribution of reinforcing material on the worn surface of MMCs, thereby affecting micro hardness (HV). Contact between the surface and counter-surface of AA-MMCs subjects the material to significant stress and distortion. Initially, micro hardness decreases due to substantial plastic deformation and grain refinement during the sliding process. However, as the SD increases, micro hardness begins to rise again, eventually stabilizing after a certain sliding distance due to the generation of in situ wear debris and re-growth of the worn surface through enhanced diffusion caused by slag impact [43].

Results of AA HCs Density

The mass density of the AA HCs was assessed using Archimedes' principle, and the findings are depicted in Table 2 as observed or actual density, while theoretical density was calculated using the rule of

mixture. Mass densities of A6061/ B₄C /Gr composites decrease with increasing reinforcement percentage, slightly falling below that of the unreinforced aluminum alloy. Notably, the AA/15% B₄C /20% Gr hybrid composite shows the lowest density among all hybrids studied. The incorporation of boron carbide and graphite particles contributes to a reduction in density, rendering the composites lightweight and suitable for automotive applications. Given that the density of boron carbide (2.51 g/cm³) and graphite (2.13 g/cm³) is lower than that of aluminum alloy (2.65 g/cm³), the resulting hybrid composites exhibit a lower overall density [33]. Three experimental trials were conducted to ensure accuracy.

Table 2. Density of A6061 and composites.

Material	Theoretical Density (g/cm ³)	Observed Density (g/cm ³)	% Deviation
AA	2.6500	2.6490	0.0377
AA/5% B ₄ C/10% Gr	2.6112	2.6083	0.1131
AA/10% B ₄ C/15% Gr	2.581	2.575	0.231
AA/10% B ₄ C/20% Gr	2.562	2.5588	0.1232
AA/15% B ₄ C/20% Gr	2.532	2.5288	0.1251

The Ultimate Compressive Strength (UCS) of A6061/ B₄C /Gr composites exhibited an increase attributed to the cushioning effect and uniform dispersion of B₄C and Gr reinforcing particles within the AA matrix alloy. With higher weight percentages of reinforcing material, the particles were better integrated into the AA matrix, resulting in reduced grain size in the microstructure. The interfacial area between B₄C and the AA matrix also expanded with increasing B₄C weight percentage, with particles tending to accumulate at these interfaces rather than at grain boundaries.

Figure 5 depicts the UCS values of A6061 with added Gr and B₄C reinforcements, showing an upward trend as the weight percentage of reinforced material increases. Notably, composites with 20% Gr and B₄C (5%, 10%, and 15%) exhibited particularly high UCS values, outperforming the base alloy. Moreover, increasing the weight percentage of Gr led to larger grain sizes, which contributed to a higher dislocation density in the AA matrix and enhanced compressive strength of the AA HCs.

The tribological characteristics of A6061/ B₄C /Gr composites are summarized in Table 3, presenting the cumulative wear values (WL) of both base metal and HC specimens after reinforcement. Dry sliding wear significantly decreased compared to the matrix metal, with lower WL values indicating reduced wear. Utilizing a Pin-on-Disk Tribometer (PODT), variations in B₄C and Gr weight percentages, applied load, sliding velocity, and sliding distance were examined. Notably, A6061/5% B₄C /10% Gr exhibited lower

WL compared to A6061/15% B₄C /20% Gr, indicating higher wear resistance. This lower WL resulted in the formation of a protective layer on the surface.

Overall, all specimens displayed a rising wear rate pattern with increasing load, especially beyond 30 N, and at a sliding velocity of four m/s. However, the wear rate remained consistent across different reinforcement percentages until reaching 40 N load, while increasing sliding velocity from 2 to 4 m/s. Scanning Electron Microscope (SEM) images revealed that wear loss increased with load exceeding 30 N due to plasticized surface debonding. Similarly, higher applied load (40 N), sliding distance, and sliding velocity resulted in increased wear loss, although the reinforced alloy demonstrated greater stability compared to the unreinforced one. Notably, the sample A6061/5% B₄C /10% Gr showed a modest 7.6% improvement in wear loss at higher loads compared to AA samples.

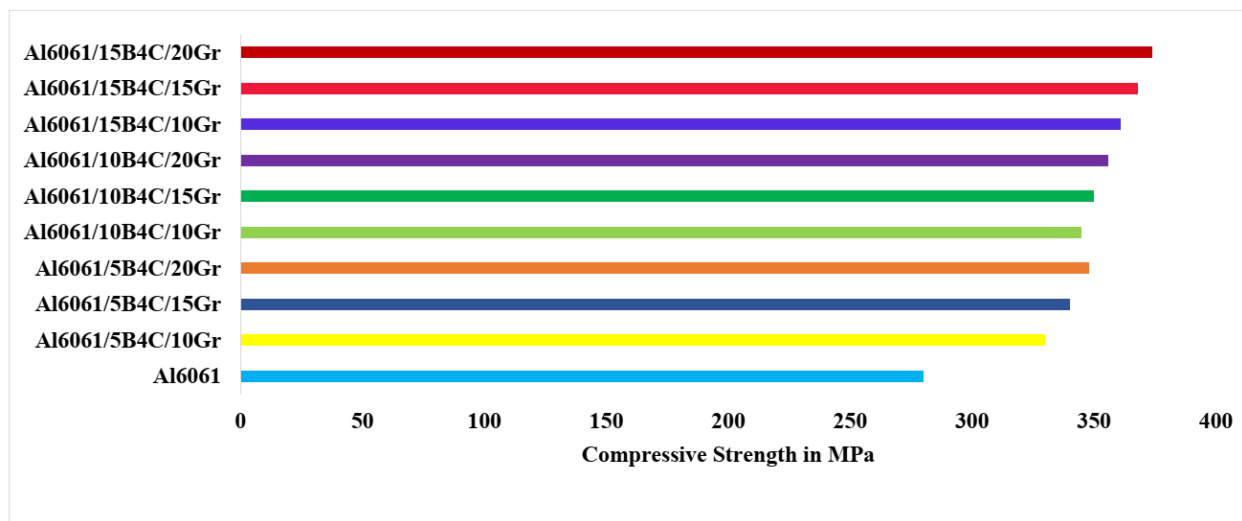


Figure 5. Compressive strength of A6061/ B₄C /Gr with varying combinations of B₄C (5, 10, and 15%) and Gr (10, 15, and 20%) HCs.

Table 3. Cumulative weight loss values of AA and Al-HC.

No.	Sliding Speed in m/s	Weight Loss in gm			
		AA	AA6061/5B ₄ C/10Gr	AA6061/10B ₄ C/15Gr	AA6061/15B ₄ C/20Gr
1	2	0.037	0.0342	0.0321	0.028
2	4	0.039	0.0359	0.0345	0.033

Micrographs of the worn surfaces of the HCs, depicted in Figure 7a–c, reveal adhesive wear after subjecting them to an applied average axial load (ANL) of 30 N, sliding a distance of 2000 m, and a sliding speed of 3 m/s. Comparative observation of the wear behavior between AA and HCs under various loads highlights distinct features. The worn surface of the AA pin exhibits more

debris accumulation, while the abraded wear surfaces of the HCs show coarse and deep grooves aligned with the sliding direction.

The application of load intensifies the formation of coarse grooves, wear debris, and surface delamination. Direct application of significant plastic stresses on the pin's surface, coupled with the abrasive action of harsh asperities on the steel counter face, results in plowing or cutting into the pin, leading to material removal in the form of tiny pieces from the matrix material.

Notably, the surface of the pin materials experiences displacement up to a radius of 0.5 mm on one side of the specimen, while the remaining surface remains relatively flat. Such fractures are typically attributed to wear debris accumulation and displacement.

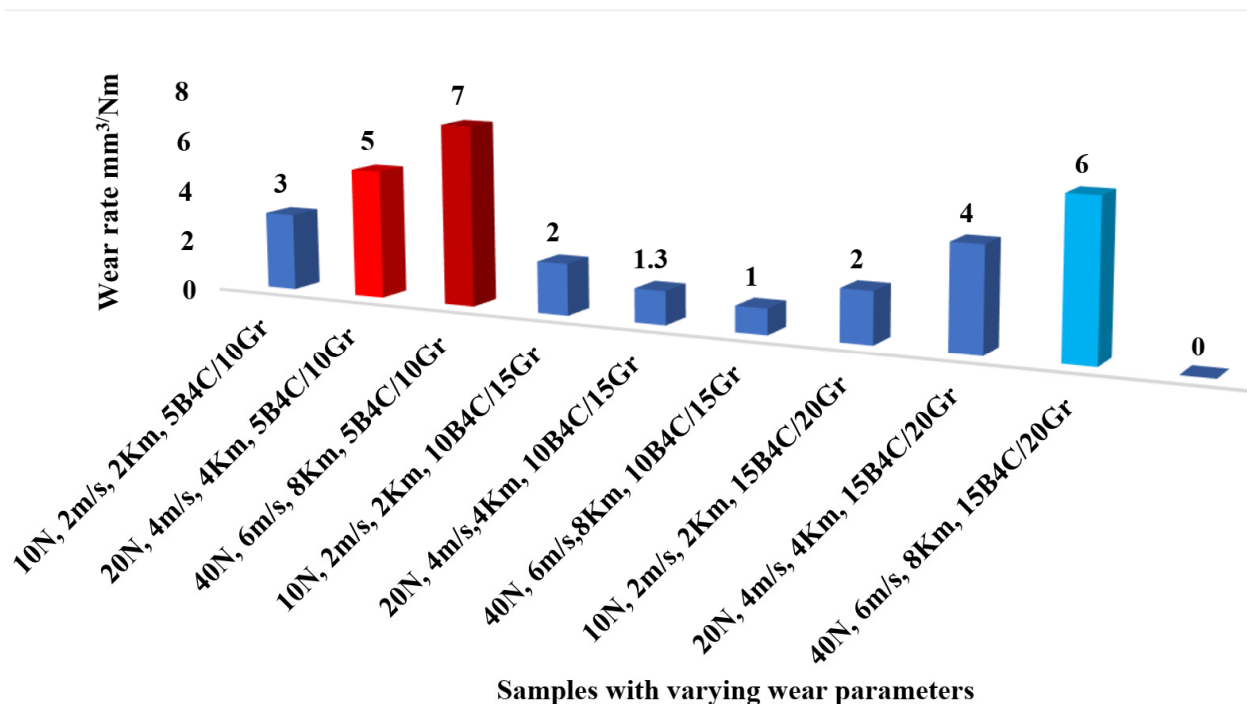
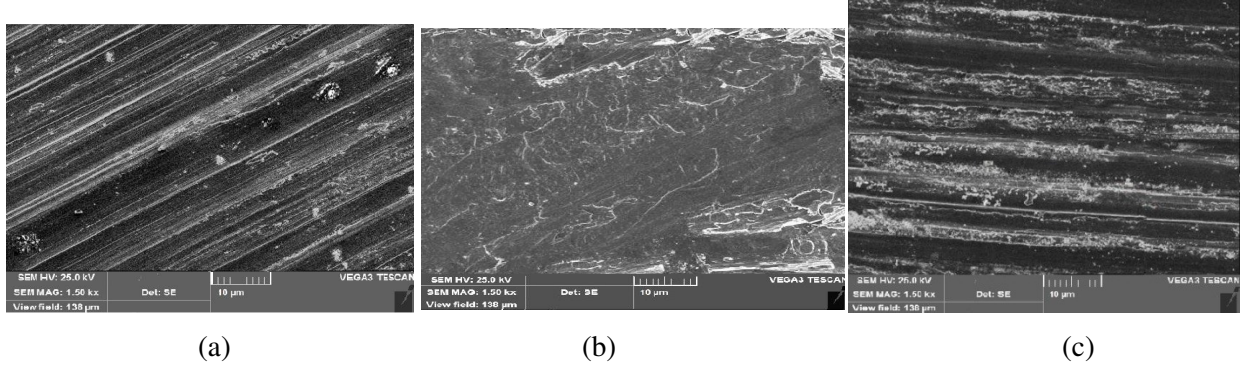


Figure 6. WR vs. load, SV, and SD for A6061/5% B₄C /10% Gr, 10% B₄C /15% Gr and 15% B₄C /20% Gr composites.



- (a) The SEM micrographs depicted in Figure 7 illustrate the worn surface morphology of A6061 reinforced with various combinations of B₄C and Gr (graphite) under specific test conditions. At a load of 30 N, a sliding speed of 3 m/s, and a sliding distance of 2000 m, the following observations were made:
- (b) For the A6061/5% B₄C 10% Gr composite, fine and shallow grooves were discernible in the sliding direction, accompanied by small debris formation. The presence of B₄C reinforcement contributed to reducing the width of the grooves and the generation of debris, resulting in decreased wear rates. The enhanced load-bearing capacity of the composite also improved its resistance to abrasion.
- (c) In the case of the A6061/10% B₄C /15% Gr composite, similar trends were observed, with reduced groove width and debris development compared to the previous composition. The incorporation of stronger B₄C reinforcement further mitigated wear rates and enhanced abrasion resistance.
- (d) With the A6061/15% B₄C /20% Gr composite, similar observations were made regarding groove width reduction and diminished debris formation compared to the other composites. The presence of higher proportions of B₄C and Gr continued to contribute to enhanced wear resistance and reduced wear rates.
- (e) Furthermore, when the applied axial load was increased to 20 N, delamination emerged as the predominant characteristic due to subsurface plastic deformation and the propagation of subsurface cracks. This led to the formation of broader grooves and an increased amount of debris. The stress induced by repetitive sliding on inclusions or flaws within the aluminum alloy initiated the nucleation of subsurface fractures, which eventually propagated parallel to the surface, resulting in the generation of long, thin flakes or plate-like debris.
- (f) In summary, the SEM observations highlight the influence of B₄C and Gr reinforcements on wear behavior under varying loads, with the composites exhibiting improved wear resistance and altered wear mechanisms compared to the base aluminum alloy.

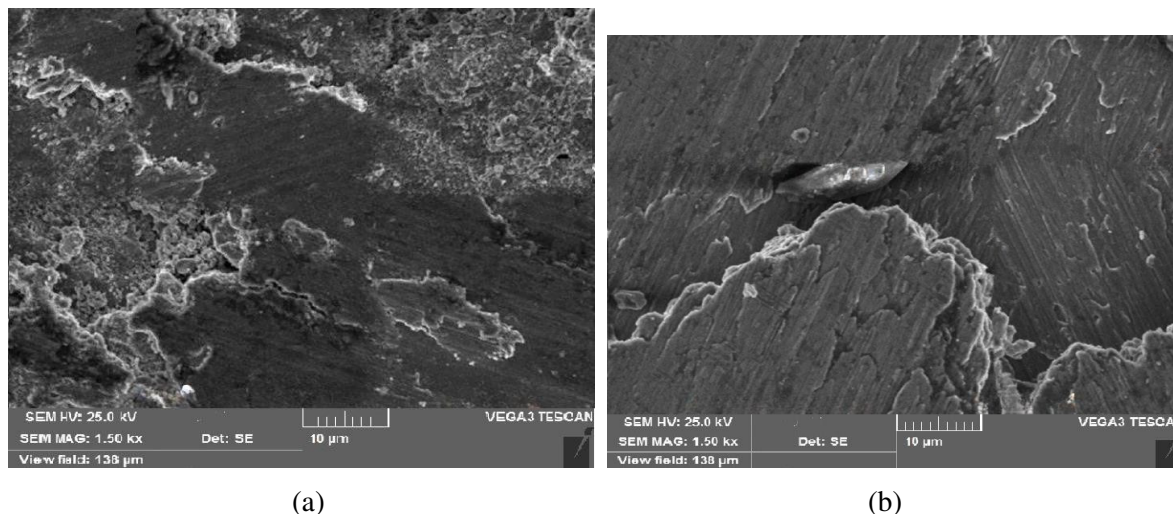


Figure 8. SEM pictures of worn-out surface of the A6061/5 B₄C /10 Gr vs. applied axial load (a) 10 N and (b) 20 N.

AA's wear rates (WRs) rose consistently as applied axial loads increased, with a particularly sharp increase at 30 N. At this load, the worn pin surface exhibited delamination, wider grooves with more debris, and a combination of adhesive and abrasive wear. Figure 7 illustrates the creation of rows of furrows on the worn pin surface (it can produce or generate holes by removing particles and covering the created holes with free particles because of the presence of two different sizes and the lubricating nature of Gr). Evidence of material transfer and plastic deformation could be observed on the pin surface. The increased load caused the breakdown of the oxide layer due to metallic contact, resulting in significant plastic deformation of the surface irregularities. Fractures were created and propagated across the asperities when the deformation in each shear band reached a critical limit, eventually removing particles from the deformed asperity. The wear resistance increased with increasing B₄C reinforcement in composites up to 10%, but wear resistance diminished when B₄C was combined over 10%. The highest wear resistance was reported in the case of HCs with AA/5 B₄C /10Gr. However, when stress increased, a higher degree of B₄C reinforcement (15%) was equal to 20% Gr reinforcement. Among all SS and load levels, the AA/15 B₄C /20Gr HC exhibited the lowest wear resistance, as shown in Figure 9a,b [33,49,50]. The applied axial load resulted in the production of fine grooves and shallow cracks in B₄C -reinforced HCs. Additionally, graphite smears and spreads across the surface under load, creating a smeared layer that functions as a lubricant. With greater load, this oxide layer and the scattered graphite layers remain stable, allowing B₄C particles to form a protective mixed matrix layer (MML), as depicted in Figure 10a,b.

The worn surfaces of the parent AA and AA/15% B₄C /20% Gr HC specimens, tested at SS of 1–3 m/s, revealed that even at a lower SS, the unreinforced parent AA displayed abrasive wear with the formation

of coarse and deep grooves in the sliding direction. As the SS increased, significant abrasive wear occurred, resulting in material pulling away from the surface, leading to loose abrasive debris. With an increased sliding speed, material removal through delamination and defoliation caused deeper and wider grooves. The thin oxide films on the unworn AA surfaces quickly degraded under the influence of abrasion, facilitating direct metallic contact between the sliding contacts and resulting in higher wear rates for AA; however, at a constant sliding speed of 3 m/s, oxide wear debris filled troughs on the pin surface, compacting into a protective layer that limited metallic contact and reduced the wear rate of AA [37,51].

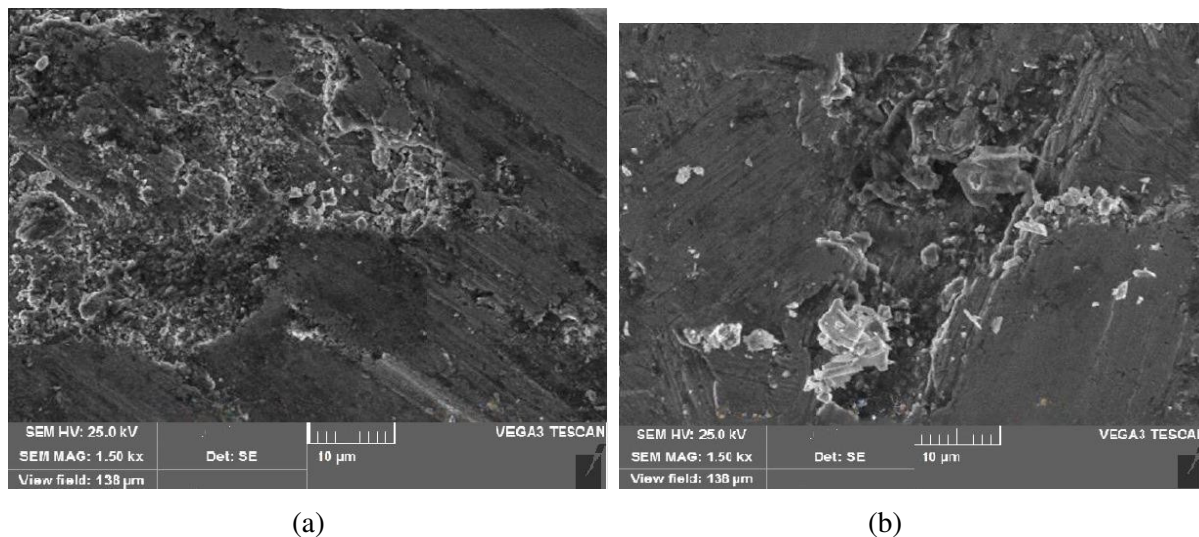


Figure 9. SEM pictures of worn-out surface of the A6061/10% B₄C /15% Gr vs. sliding speed of (a) 2 m/s and (b) 3 m/s.

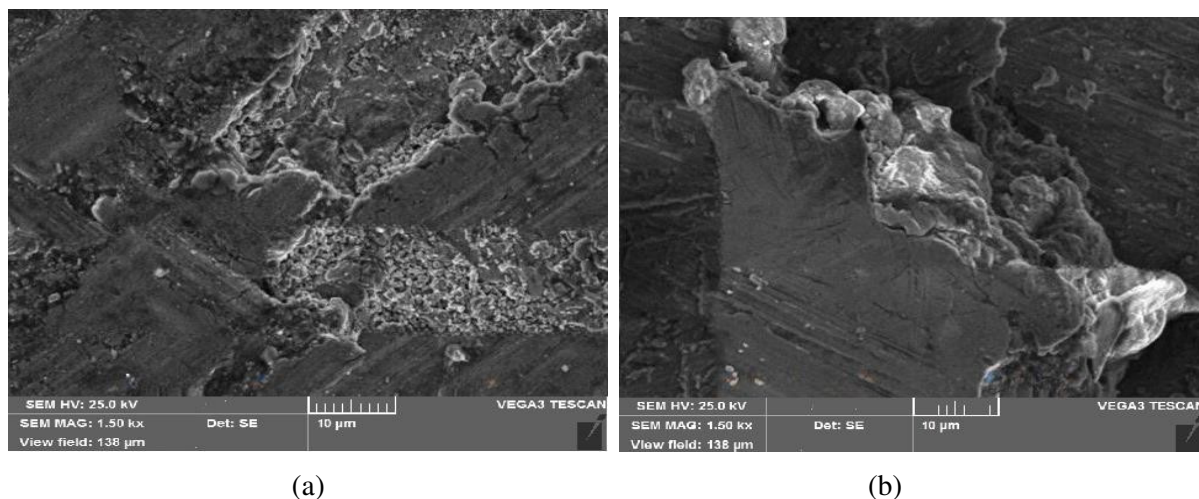


Figure 10. SEM pictures of worn-out surface of the A6061/15% B₄C /20% Gr vs. applied axial load of (a) 10 N and (b) 20 N.

Oxidative wear in AA/15% B₄C /20% Gr HCs leads to the production of mechanically mixed layers (MMLs). MMLs produce a work-hardened layer between the HC pin and the counter face, isolating the wearing surfaces and preventing asperity interactions with the pin surfaces, leading to decreases in the wear resistance of the HC. As the B₄C concentration increases, a stable MML layer forms, significantly reducing the wear rate of AA/15% B₄C/20% Gr HC compared to other composites. MML has also been observed in A6061 MMCs. As the sliding speed increases, the asperities on the softer AA surfaces deform and shatter, resulting in a smoother surface. Strain in the material beneath the worn surface reaches significant levels, although it does not immediately contribute to fracture formation. When fractures reach the surface, long and thin wear sheets separate, forming large delamination craters, as depicted in Figure 11a–c [48–54].

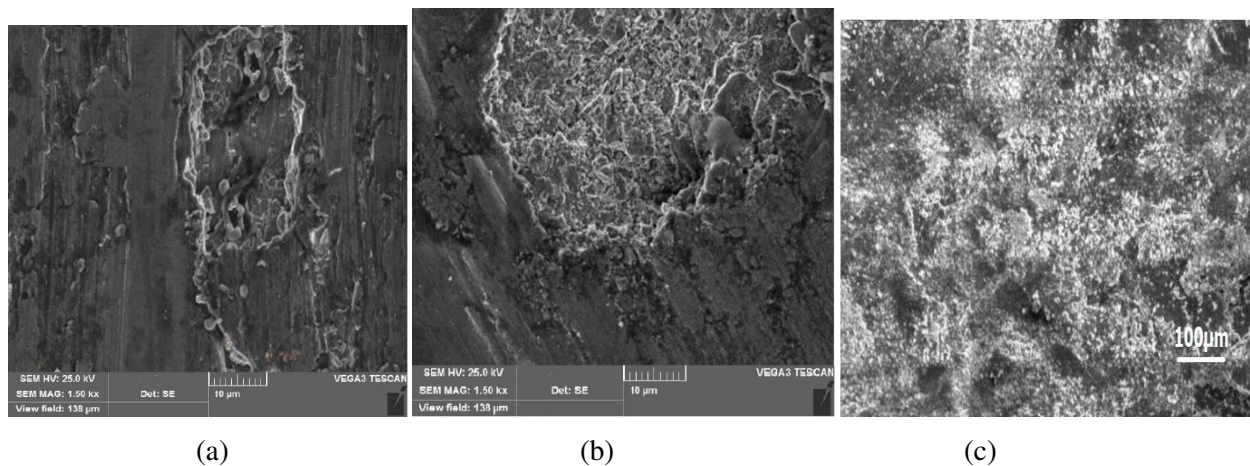


Figure 11. SEM pictures of worn-out surface of the A6061/15% B₄C /20% Gr vs. sliding speed of (a) 2 m/s and (b) 3 m/s (c) at 3 m/s with low magnification.

The coefficients of friction (COF) of composites and unreinforced alloys were calculated in order to evaluate their friction behavior. Figure 12a shows that as the applied load grew, so did the COF of the AA and their HCs. As the load rises due to wear, debris accumulation increases, which may affect the true area of contact and hence the COF. This might be because the dry sliding wear testing employed a larger load range and sliding speed. With the addition of Gr particles, the COF in A6061 alloy dropped, reaching a minimum at 15% Gr content. This is twice as cheap as the basic alloy. The addition of 15% Gr to the basal matrix material has no discernible effect on the COF. The lubricating layer thickness and Gr content both rise, lowering the COF and reducing shear stress at the subsurface. The composite has better tribological properties than the matrix alloy, keeping the wear rate and COF low at an acceptable Gr content. The existence of a smeared graphite layer at the tribosurface, serving as a solid lubricant, can be attributed to the lower COF. As the B₄C percentage is increased, the COF lowers until it reaches a minimum value for 10% of the A6061 alloy. The COF rises with further B₄C addition as a result of the

composite developing a thicker MML. Figure 12b illustrates the EDS results of the worn-out face where element Gr is missing, indicating that it might have changed phase (lubricant).

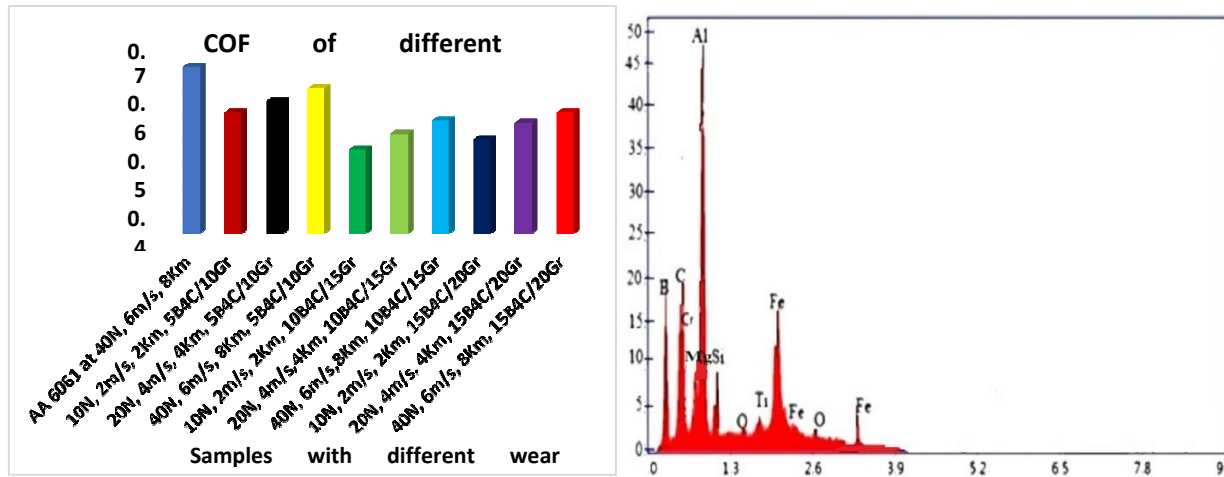


Figure 12. (a) COF of various HMMCs under variation of parameters and (b) EDS results after wear-out.

4. Conclusions

The study found that SCP was a successful method for producing A6061 HCs with B₄C and Gr reinforcing components. The reinforcing components were evenly distributed throughout the AA matrix, creating interface boundaries.

The inclusion of B₄C and Gr elements prevented dislocation and increased the material's hardness, wear resistance, and compressive characteristics.

The mixed layer containing B₄C and Gr decreased WL more effectively.

The composites with 15 vol.% B₄C and 20 vol.% Gr exhibited improved morphological, mechanical, and tribological characteristics.

Wearing resistance was found to be related to hardness. Because of the inhomogeneous distribution of reinforcing elements on the worn surface, microhardness changes with SD. The distribution of the reinforcing components was uniform throughout the AA matrix, creating interface boundaries between them.

The inclusion of B₄C and Gr elements helped to prevent dislocation.

The low wear loss and reduced COF of the composites mixed with B₄C, and Gr layers demonstrated little aggregation of reinforced material, a dispersed graphite layer functioning as a solid lubricant, and higher B₄C content producing thicker MML.

However, corrosion tests must be conducted, and future research should aim to minimize the drawbacks of these composites during machining

References

1. Singh, J.; Chauhan, A. Characterization of hybrid aluminum matrix composites for advanced applications—A review. *J. Mater. Res. Technol.* 2016, 5, 159–169.
2. Kala, H.; Mer, K.K.S.; Kumar, S. A Review on Mechanical and Tribological Behaviors of Stir Cast Aluminum Matrix Composites. *Procedia Mater. Sci.* 2014, 6, 1951–1960.
3. Bujari, S.S.; Kurahatti, R. Microstructure and Wear Behavior of B4C Particulates Reinforced Al-4.5%Cu Alloy Composites. *IOSR J. Mech Civ. Eng.* 2017, 4, 4–9.
4. Nie, C.; Gu, J.; Liu, J.; Zhang, D. Production of Boron Carbide Reinforced 2024 Aluminum Matrix Composites by Mechanical Alloying. *Composites* 2007, 48, 990–995.
5. Rohatgi, P.; Schultz, B.; Daoud, A.; Zhang, W. Tribological performance of A206 aluminum alloy containing silica sand particles. *Tribol. Int.* 2010, 43, 455–466.
6. Alizadeh, M. Effects of temperature and B4C content on the bonding properties of roll-bonded aluminum strips. *J. Mater. Sci.* 2012, 47, 4689–4695.
7. Ramesh, C.S.; Khan, A.R.A.; Ravikumar, N.; Savanprabhu, P. Prediction of wear coefficient of Al6061–TiO₂ composites. *Wear* 2005, 259, 602–608.
8. Yilmaz, O.; Buytoz, S. Abrasive wear of Al₂O₃-reinforced aluminium-based MMCs. *Compos. Sci. Technol.* 2001, 61, 2381–2392.
9. Oñoro, J.; Salvador, M.D.; Cambronero, L.E.G. High-temperature mechanical properties of aluminium alloys reinforced with boron carbide particles. *Mater. Sci. Eng. A* 2009, 499, 421–426.
10. Chegini, M.; Fallahi, A.; Shaeri, M.H. Effect of Equal Channel Angular Pressing (ECAP) on Wear Behavior of Al-7075 Alloy. *Procedia Mater. Sci.* 2015, 11, 95–100.
11. Shanbhag, V.V.; Yalamoori, N.N.; Karthikeyan, S.; Ramanujam, R.; Venkatesan, K. Fabrication, Surface Morphology and Corrosion Investigation of Al 7075-Al₂O₃ Matrix Composite in Sea Water and Industrial Environment. *Procedia Eng.* 2014, 97, 607–613.
12. Prasanna, S.C.; Ramesh, C.; Manivel, R.; Manikandan, A. Preparation of Al6061-SiC with neem leaf ash in AMMCs by using stir casting method and evaluation of mechanical, wear properties and investigation on microstructures. *Appl. Mech. Mater.* 2017, 854, 115–120.
13. Alvandi, H.; Farmanesh, K. Microstructural and Mechanical Properties of Nano/Ultra-fine Structured 7075 Aluminum Alloy by Accumulative Roll-Bonding Process. *Procedia Mater. Sci.* 2015, 11, 17–23.
14. Suresh, S.; Moorthi, N.S.V. Process Development in Stir Casting and Investigation on Microstructures and Wear Behavior of TiB₂ on Al6061 MMC. *Procedia Eng.* 2013, 64, 1183–1190.

15. Rana, H.G.; Badheka, V.J.; Kumar, A. Fabrication of Al7075/B4C Surface Composite by Novel Friction Stir Processing (FSP) and Investigation on Wear Properties. *Procedia Technol.* 2016, 23, 519–528.
16. Ramesh, C.S.; Swamy, N.R.P.; Chandrashekar, T. Effect of heat treatment on strength and abrasive wear behaviour of Al6061-SiCp composites. *Bull. Mater. Sci.* 2010, 33, 49–54.
17. Umanath, K.; Selvamani, S.T.; Palanikumar, K.; Sabarikreeshwaran, R. Dry Sliding Wear Behaviour of A6061-T6 Reinforced SiC and Al₂O₃ Particulate Hybrid Composites. *Procedia Eng.* 2014, 97, 694–702.
18. Yoo, S.C.; Kang, B.; Van Trinh, P.; Phuong, D.D.; Hong, S.H. Enhanced mechanical and wear properties of Al6061 alloy nanocomposite reinforced by CNT-template-grown core-shell CNT/SiC nanotubes. *Sci. Rep.* 2020, 10, 12896.
19. Sharif, E.M.; Karimzadeh, F.; Enayati, M.H. Fabrication and evaluation of mechanical and tribological properties of boron carbide reinforced aluminum matrix nanocomposites. *Mater. Des.* 2011, 32, 3263–3271.
20. Lawrance, C.A.; Prabhu, P.S. Stir Casting of in-situ Al 6061TiB₂ Metal Matrix Composite Synthesized with Different Reaction Holding Times. *Int. J. Eng. Res. Technol. IJERT* 2015, 4, 449–453.
21. Ren, Y.; Huang, Z.; Wang, Y.; Zhou, Q.; Yang, T.; Li, Q.; Jia, Q.; Wang, H. Friction-induced rapid amorphization in a wear-resistant (CoCrNi)₈₈Mo₁₂ dual-phase medium-entropy alloy at cryogenic temperature. *Compos. Part B Eng.* 2023, 263, 110833.
22. Alaneme, K.K.; Aluko, A.O. Production and Age-Hardening Behavior of Borax Premixed SiC reinforced Al-Mg-Si alloy Composites developed by Double Stir-Casting Technique. *West Indian J. Eng.* 2012, 34, 80–85.
23. Suresha, S.; Sridhara, B. Wear characteristics of hybrid aluminium matrix composites reinforced with graphite and silicon carbide particulates. *Compos. Sci. Technol.* 2010, 70, 1652–1659.
24. Uthayakumar, M.; Aravindan, S.; Rajkumar, K. Wear performance of Al-SiC-B₄C hybrid composites under dry sliding conditions, *Mater. Des.* 2013, 47, 456–464.
25. Kumar, V.; Raja, K.; Chandrasekar, V.S.; Thulasiram, R. Thrust force evaluation and microstructure characterization of hybrid composites (Al7075/B₄C/BN) processed by conventional casting technique. *J. Braz. Soc. Mech. Sci. Eng.* 2019, 41, 228.
26. Prabakaran S Chandramohan, G.; Sundaram, P.S. Influence of Graphite on the Hardness and Wear behavior of A6061-B₄C Composite. *Mater. Technol.* 2018, 48, 661–667.

27. Sharath, B.N.; Venkatesh, C.V.; Afzal, A.; Aslfattahi, N.; Aabid, A.; Baig, M.; Saleh, B. Multi Ceramic Particles Inclusion in the Aluminium Matrix and Wear Characterization through Experimental and Response Surface-Artificial Neural Networks. *Materials* 2021, 14, 2895.
28. Ravindranath, V.M.; Shankar, G.S.S.; Basavarajappa, S.; Kumar, N.G.S. Dry sliding Wear Behavior of Hybrid aluminum Metal Matrix composite reinforced with Boron carbide and graphite particles. *Mater. Today Proc.* 2017, 4, 11163–11167.
29. Sharath, B.; Madhu, K.; Venkatesh, C. Experimental Study on Dry Sliding Wear Behavior of Al-B4C-Gr Metal Matrix Composite at Different Temperatures. *Appl. Mech. Mater.* 2019, 895, 96–101.
30. Venkataraman, B.; Sundararajan, G. Correlation between the characteristics of the mechanically mixed layer and wear behavior of aluminium, Al-7075 alloy and Al-MMCs. *Wear* 2000, 245, 22–38.
31. Leng, J.; Jiang, L.; Wu, G.; Tian, S.; Chen, G. Effect of Graphite Particle Reinforcement on Dry Sliding Wear of SiC/Gr/Al Composites. *Rare Met. Mater. Eng.* 2009, 38, 1894–1898.
32. Nagaraju, S.B.; Somashekara, M.K.; Puttegowda, M.; Manjulaiah, H.; Kini, C.R.; Venkataramaiah, V.C. Effect of B4C/Gr on Hardness and Wear Behavior of Al2618 Based Hybrid Composites through Taguchi and Artificial Neural Network Analysis. *Catalysts* 2022, 12, 1654.
33. Ramanathan, A.; Krishnan, P.K.; Muraliraja, N. A review on the production of wear resistance model for the metal matrix composites, through stir casting, furnace design, properties, challenges, and research opportunities. *J. Manuf. Process.* 2019, 42, 213–245.
34. Thiyagarajan, T.; Subramanian, R.; Somasundaram Dharmalingam Achiappan Radhika, N.; Gowrisankar, A. Wear behavior of B4C reinforced hybrid aluminum matrix composites. *Mater. Technol.* 2014, 46, 497–501.
35. Baradeswaran, A.; Vettivel, S.C.; Perumal, A.E.; Selvakumar, N.; Issac, R.F. Experimental investigation on mechanical behavior, modelling and optimization of wear parameters of B4C and graphite reinforced aluminium hybrid composites. *Mater. Des.* 2014, 63, 620–632.
36. ASTM E384-10; Standard Test Method for Microindentation Hardness of Materials. ASTM: West Conshohocken, PA, USA, 2010.
37. Thirumalai, T.; Subramanian, R.; Kumaran, S. Production and characterization of hybrid aluminum matrix composites reinforced with boron carbide (B4C) and graphite. *J. Sci. Ind. Res.* 2014, 73, 667–670.
38. ASTM-E9; International. Standard Test Methods of Compression Testing of Metallic Materials at Room Temperature. ASTM: West Conshohocken, PA, USA, 2009.

39. Karthe, M.; Karuppusamy, S.; Sureshkumar, B.; Ali, A.N. Mechanical and wear properties of Al7075-B4C–Gr metal matrix composites fabricated by the using stir casting method. *Mater. Today Proc.* 2023, 77, 389–393.
40. ASTM G99-17; Standard Test Method for Wear Testing with a Pin-on-Disk Apparatus. ASTM: West Conshohocken, PA, USA, 2017.
41. Narayan, S.; Rajeshkannan, A. Hardness, tensile and impact behaviour of hot forged aluminium metal matrix composites. *J. Mater. Res. Technol.* 2017, 6, 213–219.
42. Bodunrin, M.O.; Alaneme, K.K.; Chown, L.H. Aluminium matrix hybrid composites: A review of reinforcement philosophies; mechanical, corrosion and tribological characteristics. *J. Mater. Res. Technol.* 2015, 4, 434–445.
43. Ramadoss, N.; Pazhanivel, K.; Anbuechezhiyan, G. Synthesis of B4C and BN reinforced Al7075 hybrid composites using stir casting method. *J. Mater. Res. Technol.* 2020, 9, 6297–6304.
44. Nasr, A.A. Thermal protection of a vertical plate using ethylene glycol film cooling flowing down on a vertical plate. *J. Umm Al-Qura Univ. Eng. Archit.* 2023, 14, 135–141.
45. Shorowordi, K.M.; Laoui, T.; Haseeb, A.S.M.A.; Celis, J.P.; Froyen, L. Microstructure and interface characteristics of B4C, SiC and Al2O3 reinforced Al matrix composites: A comparative study. *J. Mater. Process. Technol.* 2003, 142, 738–743.
46. Basavarajappa, S.; Chandramohan, G. Wear Studies on Metal Matrix Composites: A Taguchi Approach. *J. Mater. Sci. Technol.* 2009, 21, 845–850.
47. Canakci, A.; Arslan, F.; Yasar, I. Pre-treatment process of B4C particles to improve incorporation into molten AA2014 alloy. *J. Mater. Sci.* 2007, 42, 9536–9542.
48. Patdar, D.; Rana, R.S. Effect of B4C particle reinforcement on the various properties of aluminium matrix composites: A survey paper. *Mater. Today Proc.* 2017, 4, 2981–2988.
49. Alam, M.T.; Ansari, A.H. X-ray diffraction analysis and microstructural examination of Al-SiC composite fabricated by stir casting. *Int. J. Sci. Technol. Manag.* 2015, 4, 941–956.
50. Singh, N.; Belokar, R.M. Tribological behavior of aluminum and magnesium-based hybrid metal matrix composites: A state-of-art review. *Mater. Today Proc.* 2021, 44, 460–466.
51. Baradeswaran, A. Elaya Perumal Influence of B4C on the tribological and mechanical properties of Al 7075-B4C composites. *Compos. Part B Eng.* 2013, 54, 146–152.
52. Sharma, S.; Goyal, A.; Bharadwaj, P.; Oza, A.D.; Pandey, A. Application of metal matrix composite fabricated by reinforcement materials—A review. *Mater. Today Proc.* 2023, in press.
53. Yang, H.; Jiang, L.; Balog, M.; Krizik, P.; Schoenung, J.M. Reinforcement Size Dependence of Load Bearing Capacity in Ultrafine- Grained Metal Matrix Composites. *Metall. Mater. Trans. A* 2017, 48, 4385–4392.

54. Softah, G.J. Characterization and Performance Study of DCMD in Different Configurations after Membrane Thermal 505 Treatment. J. Umm Al-Qura Univ. Eng. Archit. 2020, 11, 33–38.